American Journal of Engineering and Applied Sciences

Original Research Paper

Nonlinear Control of Variable wind Speed Conversion System Based on a Squirrel Cage Induction Generator (SCIG)

Abouobaida Hassan

Department of Electrical Engineering, Ecole Mohammadia D'ingénieurs, Mohammed V University, Rabat, Morocco

Article history
Received: 24-10-2014
Revised: 20-12-2014
Accepted: 02-01-2015

Abstract: This study presents a control strategy for a Squirrel Cage Induction Generator (SCIG)-based wind energy conversion system. Control strategies of the AC/DC/AC converter is presented along with the mathematical modeling of the employed configuration. The maximum power point extraction of the wind turbine is addressed along with the proposed strategy. The backstepping approach is introduced to control the generator speed and regulate the flux. The wind system is then simulated in MATLAB-SIMULINK and the developed model is used to illustrate the behavior of the system. The simulation results are presented and discussed at the end of this study.

Keyword: Squirrel Cage Induction Generator (SCIG), Grid Power, Unity Power Factor, Wind Energy Conversion System, Maximum Power Point Extraction

Introduction

The growing need for electrical energy and the will to preserve the nature justifies the use of renewable energy sources. The use of renewable sources for electric power generation has been a huge increase since the past decade. Increased economical and ecological woes have driven researchers to discover newer and better means of generating electrical energy. In this race, the production of electricity by wind turbine is actually the best method in comparison with the energy produced by the solar source conversion and this is due to the price per a kilo watt that is less elevated with respect to the second (Suebkinorn and Neammanee, 2011). Among the most used and available technologies for wind turbines, the Doubly Fed Induction Generator (DFIG) is the most accepted because it presents greater benefits for a reduced conversion structure and efficient energy capture due to variable speed operation.

Different types of electric generators are used for the generation of electric energy from wind. These include the Squirrel Cage Induction Generators (SCIG), the Doubly Fed Induction Generator (DFIG) and the Synchronous Generator (SG) (Suebkinorn and Neammanee, 2011).

The Squirrel Cage Induction Generator (SCIG) is suitable for alternative energy source applications because it is cheap, has simple construction, good power/weight ratio, low maintenance levels and it is robust and easily replaceable. For these reasons, the SCIG is being strongly considered as a good option in conjunction with the variable speed wind turbines (Trapp *et al*., 2012).

Variable-speed wind turbines are advantageous for their potential capability of extracting more energy from wind resources. Thus, an MPPT control strategy is necessary to adjust the turbine rotor speed according to the variation of wind speeds so that the tip speed ratio can be maintained at its optimal value.

Several MPPT control algorithms have been proposed in the technical literature. The search control such as Perturb and Observe (P&O), anemometer-based method and the fuzzy-logic based algorithms are easily implemented and are independent of wind turbine characteristics. In the P&O algorithm, the turbine speed is varied in small steps and the corresponding change in power is observed. Step changes are effected in a direction so as to move toward MPP. This process is continued until MPP is reached. By using this algorithm, maximum power corresponding to any wind velocity can be captured. But the time taken to reach MPP is long and a considerable amount of power loss takes place during the tracking phase. The anemometer-based MPPT algorithm, the wind velocity is measured and a reference speed for the induction generator corresponding to the Maximum Power Point (MPP) of the present wind velocity is set. Although this is a fast MPPT scheme, the overall cost of the system increases because anemometer is expensive. Fuzzy-control-based scheme is good, but is

complex to implement. Neural networks could be an alternative approach for the MPPT control, but the requirement for offline training in order to learn the turbine characteristics might be a considerable drawback for several installations. An optimal torque controller that follows a quadratic relation between turbine torque and speed can provide faster dynamic response, however, it needs a priori knowledge of the turbine characteristics (Mesemanolis and Mademlis, 2013).

In the grid-connected system, however, any amount of power generated by the wind energy based (SCIG) can be injected into the grid. Hence, at any wind velocity, the system can be operated at MPP to maximize the generation and utilization of power. The block diagram of a typical grid-connected wind energy conversion system is shown in Fig. 1. The transfer of the power produced by this system is made by two cascaded converters. The first is linked to the network operates as a rectifier and the second operates as an inverter is connected to the grid (Manaullah *et al*., 2012).

In this study, the problem of controlling AC/DC converter is approached using the backstepping technique. While feedback linearization methods require precise models and often cancel some useful nonlinearity, backstepping designs offer a choice of design tools for accommodation of uncertain nonlinearities and can avoid wasteful cancellations.

The backstepping approach is applied to a specific class of switched power converters, namely ac-to-dc converters. In the case where the converter model is fully known the backstepping nonlinear controller is shown to achieve the control objectives i.e., speed and flux control of (SCIG) with respect to wind change. The desired speed is designed online using a an estimate of the speed reference corresponding to operation at maximum power generator wind power. The proposed strategy ensures that the MPP is determined, the generator speed is controlled to its reference value and the close loop system will be asymptotically stable. The stability of the control algorithm is analysed by Lyapunov approach.

This study is structured as follows. Section II presents the modeling of the SCIG system. The detailed control strategy is discussed in section III. Section IV presents and discusses simulation and results followed by conclusions in section V.

Wind Energy Conversion System Modeling

The wind turbine modeling is inspired from (Manaullah *et al*., 2012). In the following, the wind turbine components models are briefly described.

The Turbine Model

The aerodynamic power P captured by the wind turbine is given by Equation 1:

$$P = \frac{1}{2}\pi\rho R^2 Cp(\lambda)v^3 \tag{1}$$

where, the tip speed ratio λ is given by Equation 2:

$$\lambda = \frac{R\omega}{v} \tag{2}$$

And v is the wind, ρ is the air density, R is the rotor radius and Cp is the power coefficient. λ is the ratio of turbine blades tip speed to wind speed and β is the turbine blades rotational speed. The Generator power as a function of generator speed for different velocity is illustrated in Fig. 2.

The rotor power (aerodynamic power) is also defined by Equation 3:

$$P = T_m.\omega \tag{3}$$

where, T_m is the aerodynamic torque and ω is the wind turbine rotor speed.

The following simplified model is adopted for the turbine Equation 4:

$$J\frac{d\omega}{dt} = T_m - T_{em} - K.\omega \tag{4}$$

Where:
T_{em} = The generator electromagnetic torque
J = The turbine total inertia
K = The turbine total external damping

The SCIG Model

The control system is usually defined in the synchronous *d-q* frame fixed to either the stator voltage or the stator flux. For the proposed control strategy, the generator dynamic model written in a synchronously rotating frame *d-q*.

The voltages of the windings of the stator and the rotor according to the *d-q* axes are given by the following relations (Kedjar and Al-Haddad, 2012):

$$\begin{cases} v_{sd} = R_s i_{sd} + \dfrac{d\Phi_{sd}}{dt} - \omega_s.i_{sq} \\ v_{sq} = R_s i_{sq} + \dfrac{d\Phi_{sq}}{dt} + \omega_s.i_{sd} \\ v_{rd} = 0 = R_r i_{rd} + \dfrac{d\Phi_{rd}}{dt} - \omega_r.i_{rq} \\ v_{rq} = 0 = R_r i_{rq} + \dfrac{d\Phi_{rq}}{dt} + \omega_r.i_{rd} \end{cases} \tag{5}$$

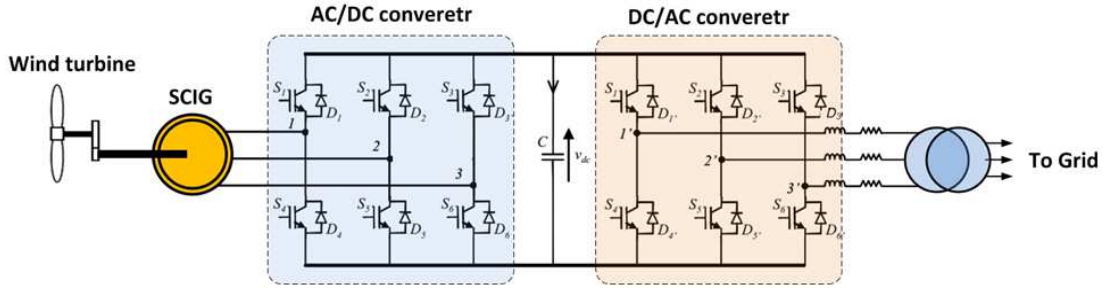

Fig. 1. SCIG-based wind energy conversion system

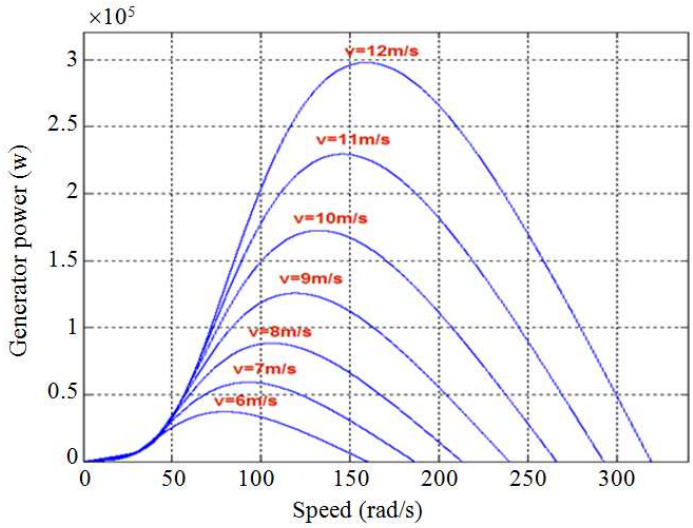

Fig. 2. Generator power as a function of generator speed for different wind speeds

The magnetic flux created by the windings of the stator and the rotor are given by the following relations:

$$\begin{cases} \Phi_{sd} = L_s I_{sd} + m.L_m.I_{rd} \\ \Phi_{sq} = L_s I_{sq} + m.L_m.I_{rq} \\ \Phi_{rd} = L_r I_{rd} + m.L_m.I_{sd} \\ \Phi_{rq} = L_r I_{rq} + m.L_m.I_{sq} \end{cases} \quad (6)$$

Where:

v	=	The voltage i the current
Φ	=	The flux
R	=	The resistance
L	=	Inductance
M	=	The mutual inductance
T_{em}	=	The electromagnetic torque
P	=	The pole pair number
L_m and m (M=$m.L_m$)	=	Magnetizing inductance and turns ratio of the stator current and rotor current respectively

The above model (5) to (7) can be presented as differential equations for the stator currents and rotor flux vector components under the following form:

$$\begin{cases} \dot{x}_1 = a_1\left(x_2.x_3 - x_7.\dot{x}_4\right) - a_2.x_1 - a_3.x_8 \\ \dot{x}_2 = -a_4.x_2 - a_5.x_4 + a_5.x_7 - a_7.x_1.x_3 + a_8.x_6 \\ \dot{x}_3 = a_9.x_4 - a_{10}.x_3 + a_5.x_7 - a_{11}.x_1.x_7 \\ \dot{x}_4 - a_4.x_4 + a_5.x_2 + a_6.x_3 + a_7.x_1.x_7 + a_8.x_5 \end{cases} \quad (7)$$

Where:

$$a_1 = \frac{P.M}{J.L_r}; a_2 = \frac{f}{J}; a_3 = \frac{1}{J};$$

$$a_4 = \frac{L_r^2.R_s + L_m^2.R_r}{\sigma.L_s.L_r^2}; a_5 = 1; a_6 = \frac{R_r.M}{\sigma.L_s.L_r^2}$$

$$a_7 = \frac{R_r.P}{\sigma.L_s.L_r}; a_8 = \frac{1}{\sigma.L_s}; a_9 = \frac{R_r.M}{L_r};$$

$$a_{10} = \frac{R_r}{L_r}; a_{11} = P$$

And:

$$x_1 = \omega_m; x_2 = i_{sq}; x_3 = \phi_{rd}; x_4 = i_{sd};$$

$$x_5 = v_{sd}; x_6 = v_{sq}; x_7 = \phi_{rq}; x_8 = T_m$$

Controls the electromagnetic torque and rotor direct flux will be obtained by controlling the dq-axes stator currents of the SCIG.

By choosing the two-phase dq related to rotating rotor field and placing the rotor flux vector on the d-axis, we have $\phi_{rd} = \phi_{rd} = \phi_r$ and $\phi_{rq} = 0$. In this case, the model (9) becomes Equation 8:

$$\begin{cases} \dot{x}_1 = a_1.x_2.x_3 - a_2.x_1 - a_3.x_8 \\ \dot{x}_2 = -a_4.x_2 - a_5.x_4 - a_7.x_1.x_3 + a_8.x_6 \\ \dot{x}_3 = a_9.x_4 - a_{10}.x_3 \\ \dot{x}_4 - a_4.x_4 + a_5.x_2 + a_6.x_3 + a_8.x_5 \end{cases} \quad (8)$$

Modeling Three-Phase Inverter

In this section, we focus on the modeling of the DC/AC inverter connected to power grid via the RL filter as illustrated in Fig. 4.

The model of the three-phase grid connected DC/AC converter is presented by the following Equation 9 (Mehdi *et al*., 2013):

$$\begin{cases} v_{s1} = v_{g1} + R_g.i_{g1} + L_g.\dfrac{di_{g1}}{dt} \\ v_{s2} = v_{g2} + R_g.i_{g2} + L_g.\dfrac{di_{g2}}{dt} \\ v_{s3} = v_{g3} + R_g.i_{g3} + L_g.\dfrac{di_{g3}}{dt} \end{cases} \quad (9)$$

The dynamic of the DC bus voltage is given by the following Equation 10:

$$c.\frac{dV_{dc}}{dt} = i_{rec} - i_{ond} \quad (10)$$

Control Strategy

The architecture of the controller is shown in Fig. 4. It is based on the three-phase model of the electromechanical conversion chain of the wind system (Mehdi *et al*., 2013).

The control strategy has three objectives:

- Control of AC/DC converter to extract maximum wind power by controlling the electromagnetic torque and d-axis flux of rotor of SCIG
- Control of the DC/AC by controlling the DC bus voltage, active and reactive power Injected to electrical network

MPPT Strategy

The control objective is to optimize the capture wind energy by tracking the optimal generator speed ω_m*.

The optimum speed which corresponds to operation at maximum power is approximated according to the wind speed Equation 11:

$$\omega_m^* = a0 + a1.v + a2.v^2 \quad (11)$$

With:

$$a0 = 16; a1 = 9.33; a2 = 0.2222$$

Control of the AC/DC Converter

In order to extracting maximum power from turbine, mechanical speed and rotor flux, two state variables have been proposed for describing the (SCIG) model as follows:

$$\dot{x}_1 = a_1\left(x_2.x_3 - x_7.x_4\right) - a_2.x_1 - a_3.x_8 \quad (12)$$

$$\dot{x}_3 = a_9.x_4 - a_{10}.x_3 + a_5.x_7 - a_{11}.x_1.x_7 \quad (13)$$

Therfore, the errors are defined using the rotational speed and rotor flux Equation 14 and 15:

$$e_1 = x_1 - x_1^* \quad (14)$$

$$e_3 = x_3 - x_3^* \quad (15)$$

In Equation 12 and 13, x_2 and x_4 behaves as a virtual control input. Such an equation shows that one gets $\dot{e}_1 = -k_1.e_1$ and $\dot{e}_3 = -k_3.e_3$ (k_1>0; k_3>0 being a design parameters) provided that Equation 16 and 17:

$$x_2 = (a_2.x_1 + a_3.x_8. - k_1e_1) / a_1.x_3 \quad (16)$$

$$x_4 = (a_{10}.x_3 - k_3e_3) / a_9 \quad (17)$$

As x_2 and x_4 are just a variables and not (an effective) control inputs, (12)-(13) cannot be enforced for all $t \geq 0$. Nevertheless, Equation 18 and 19 shows that the desired value for the variable x_2 and x_4 are respectively:

$$x_2^* = (a_2.x_1 + a_3.x_8. - k_1e_1) / a_1.x_3 \quad (18)$$

$$x_4^* = (a_{10}.x_3 - k_3e_3) / a_9 \quad (19)$$

Indeed, if the errors Equation 20 and 21:

$$e_2 = x_2 - x_2^* \quad (20)$$

$$e_4 = x_4 - x_4^* \quad (21)$$

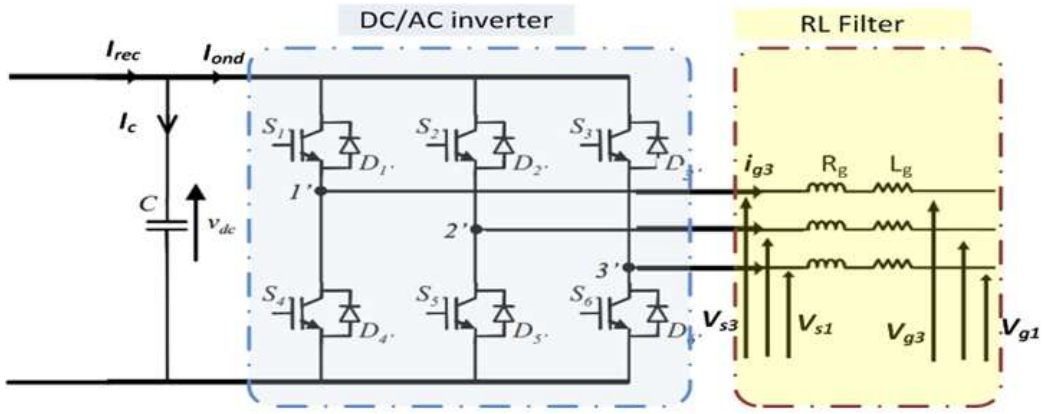

Fig. 3. Three-phase DC/ACinverter

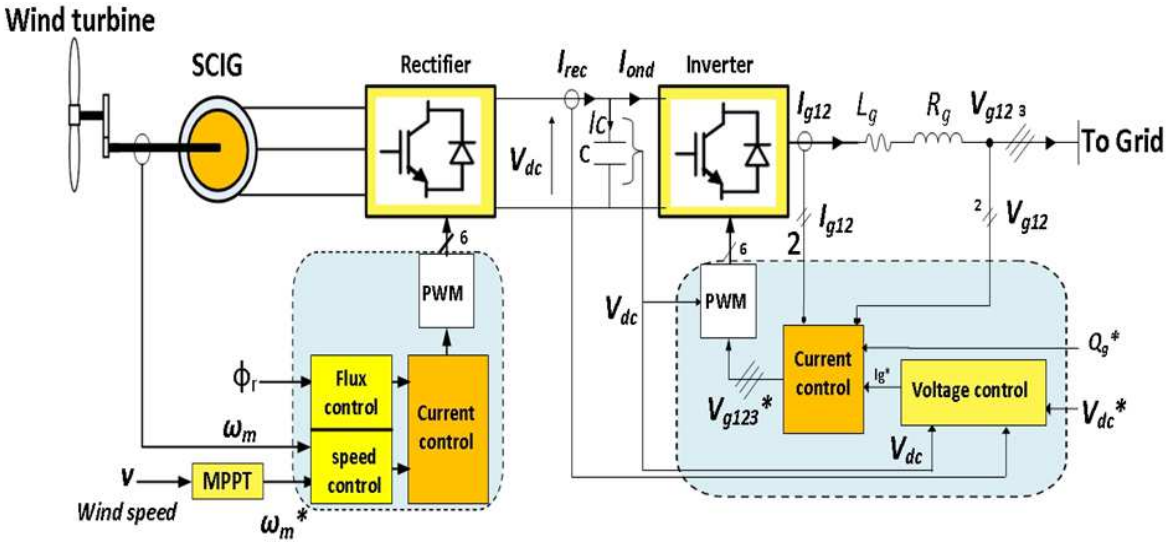

Fig. 4. Control strategy

The desired value x_2^* and x_2^* are called a stabilization function.

Deriving e_1 and e_3 with respect to time and accounting for (12)-(13)-(18) and (19), implies Equation 22 and 23:

$$\dot{e}_1 = -k_1.e_1 + a_3.x_3.e_2 \tag{22}$$

$$\dot{e}_1 = -k_3.e_3 + a_9.e_4 \tag{23}$$

The Lyapunov function is defined as Equation 24:

$$V = \frac{e_1^2}{2} + \frac{e_2^2}{2} + \frac{e_3^2}{2} + \frac{e_4^2}{2} \tag{24}$$

The time derivative of Lyapunov function V is given by Equation 25:

$$\dot{V} = e_1.\dot{e}_1 + e_2.\dot{e}_2 + e_3.\dot{e}_2 + e_4.\dot{e}_4 \tag{25}$$

The time-derivative of the latter, along the (e_1,e_2,e_3,e_4) trajectory is Equation 26:

$$\dot{V} = -k_1.e_1^2 - k_2.e_2^2 - k_3.e_3^2 - k_4.e_4^2 \le 0 \tag{26}$$

Then, the control $(x_5^* = v_{sd}^*, x_6^* = x_{sq}^*)$ laws are derived Equation 27 and 28:

$$x_5^* = \left(-a_9.e_3 + a_4.x_4 - k_4e_4 - a_6.x_3 - \dot{a}_5.x_2 + x_4^*\right) / a_8 \tag{27}$$

$$x_6^* = (-a_3.e_1.x_3 + a_4.x_2 + a_5.x_4 - k_2e_2 + a_7.x_1.x_3 + \dot{x}_2^*) / a_8 \tag{28}$$

DC/AC Control Strategy

The three-phase grid connected inverteris controled to:

- Regulating the dc bus voltage
- Provide a power factor close to unity (network current in phase with the network voltage)

Applying *dq* transformation and developing the equations system (9), it is possible to find the differential Equation 29:

$$\begin{cases} v_d = R_g i_d + L_g \dfrac{di_d}{dt} + L_g.\omega.i_q + v_{gd} \\ v_q = R_g i_q + L_g \dfrac{di_q}{dt} + L_g.\omega.i_d + v_{gq} \end{cases} \quad (29)$$

where, (v_{gd},v_{gq}) are the direct and quadrature components of the grid voltage respectively. (i_d,i_q) are the direct and quadrature components of the grid current.

The term $\omega.L_g.i_q + v_{gd}$ and $-\omega.L_g.i_d+v_{gq}$ are compensated by a feed-forward action. By applying the Laplace transform to the compensated system, the transfer function of the inverter is given as Equation 30:

$$G_i(p) = \frac{v_d}{i_d} = \frac{v_q}{i_q} = \frac{1}{L_g.p + R_g} \quad (30)$$

where, v_d and v_q are the inputs inverter voltages and the i_d and i_q are the outputs currents respectively.

The DC bus dynamics is given as Equation 31:

$$c.\dot{V}_{dc} = i_{rec} - i_{ond} \quad (31)$$

The application of the Laplace transform to (24) result in Equation 32:

$$c.p.\bar{V}_{dc} = i_{rec} - i_{ond} \quad (32)$$

The term i_{rec} is a disturbance in the control. It is assumed in this study that the DC bus loop is sufficiently fast, as to eliminate the perturbation term. For this reason, the DC bus function will be Equation 33:

$$G_u(p) = \frac{V_{dc}}{i_{ond}} = -\frac{1}{c.p} \quad (33)$$

The control loops of the inverter are shown in Fig. 5. Externally, there is the reactive power loop that controls the power factor and the loop to regulate the DC bus voltage. The current control loops use proportional-integral controllers. The controller gains are adjusted by the poles allocation method (Dinghui *et al*., 2009).

Simulation Results

The model of the wind turbine system based (SCIG) is built using MATLAB\SIMULINK. The parameters of the turbine and (SCIG) are given in the Table 1.

Table 1. Parameters of the turbine and (SCIG)

System	Parameter
Turbine	Jt = 50 kg.m^2,
	Vt_n = 12 m/s, R = 14 m
Multiplier	Mu = 46
SCIG	$U_s = U_r$ = 575V, P_n = 300 Kw,
	ω_n = 160 rad/s, f = 50 Hz,
	R_r = 46 mΩ, R_s = 63 mΩ,
	M= 11.6 mH, L_s = 11.8 mH,
	L_r = 11.8 mH, P = 2
DC BUS	C = 20 mF, V_{dc} = 1000 V
RL Filter	R_g = 0.1 Ω, L_g = 0.6 mH
GRID	U_g = 575 V, f = 50 Hz

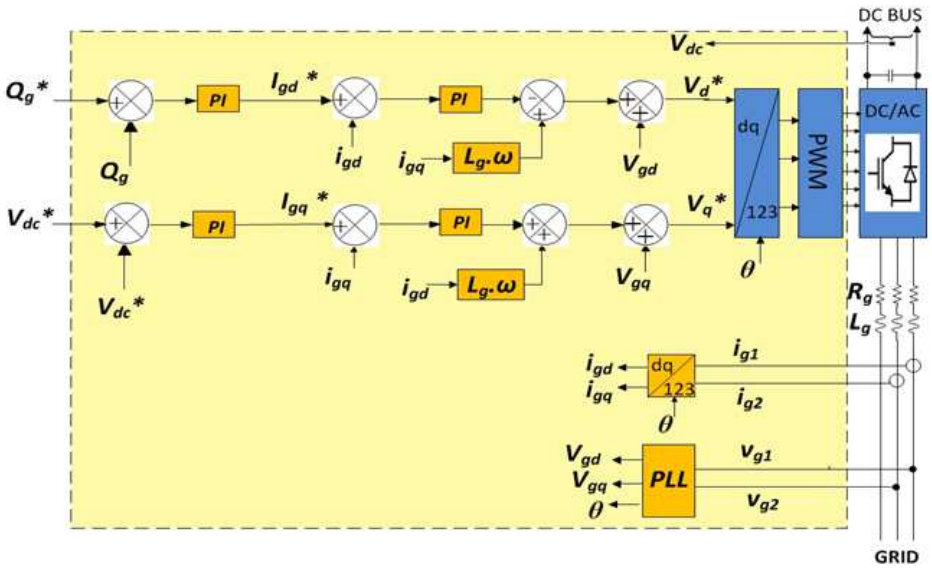

Fig. 5. Control strategy of the grid connected DC/AC converter

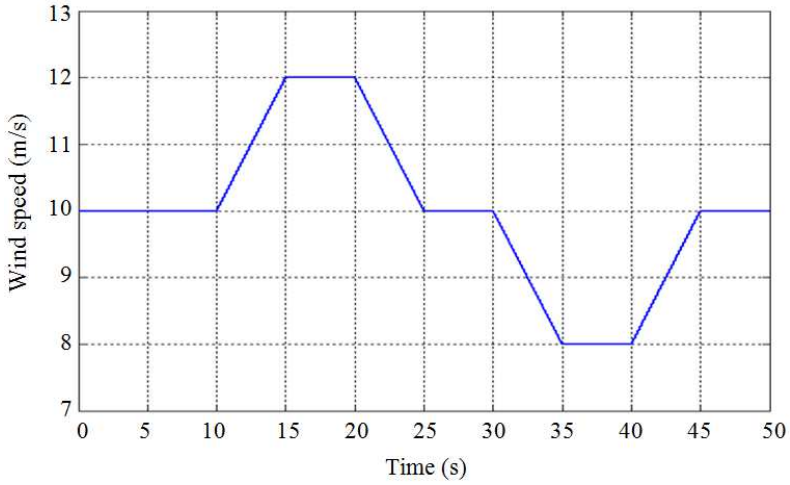
Wind speed (m/s)
Time (s)

(a)

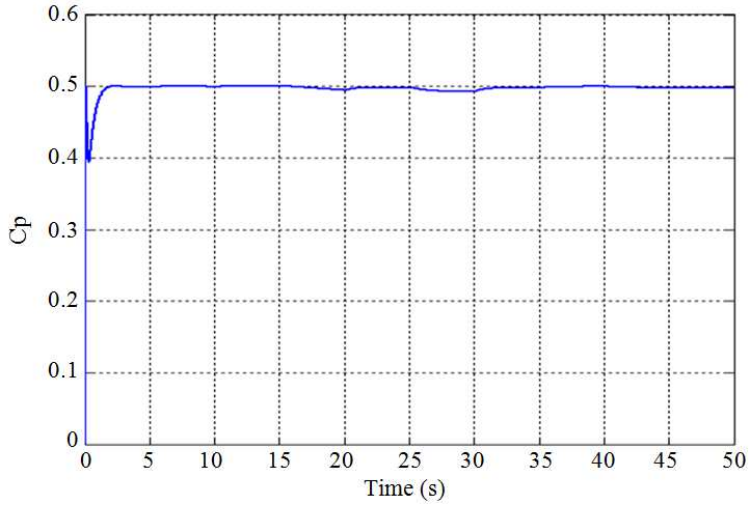
Cp
Time (s)

(b)

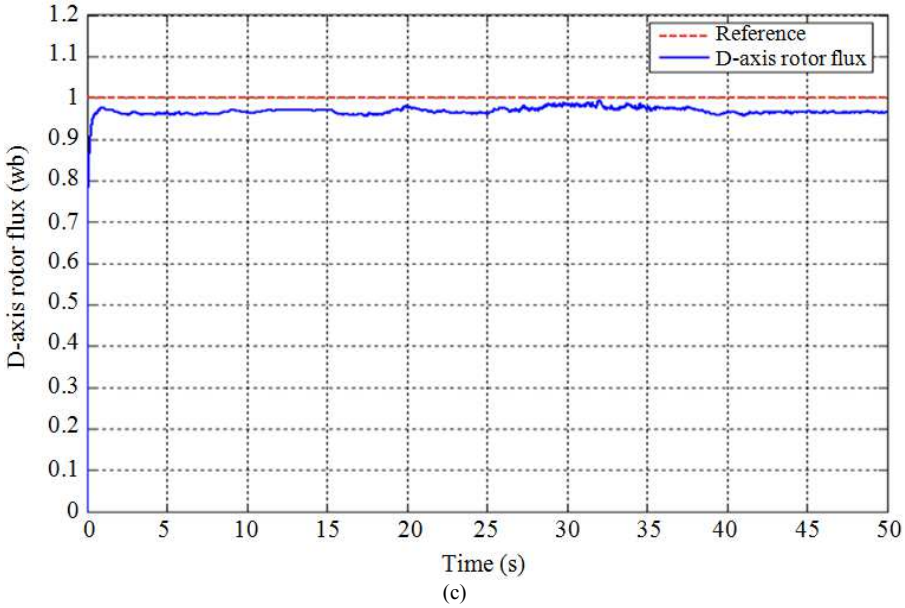
Reference
D-axis rotor flux
D-axis rotor flux (wb)
Time (s)

(c)

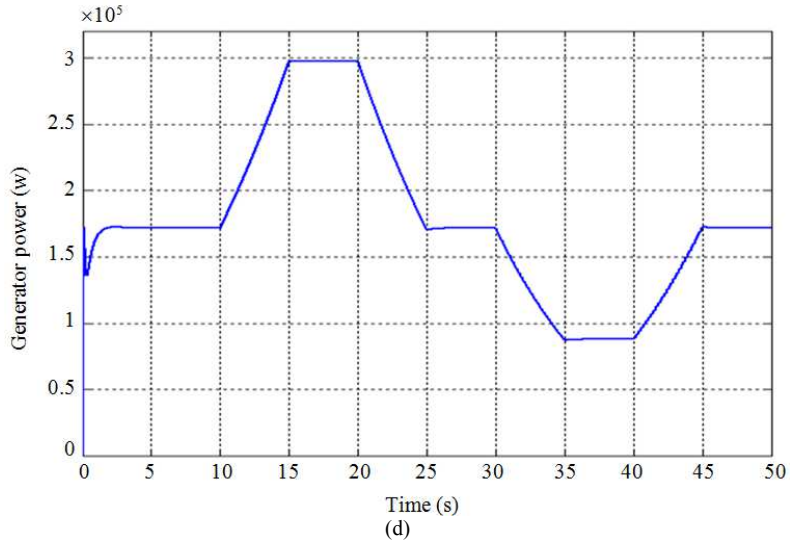
×10^5
Generator power (w)
Time (s)

(d)

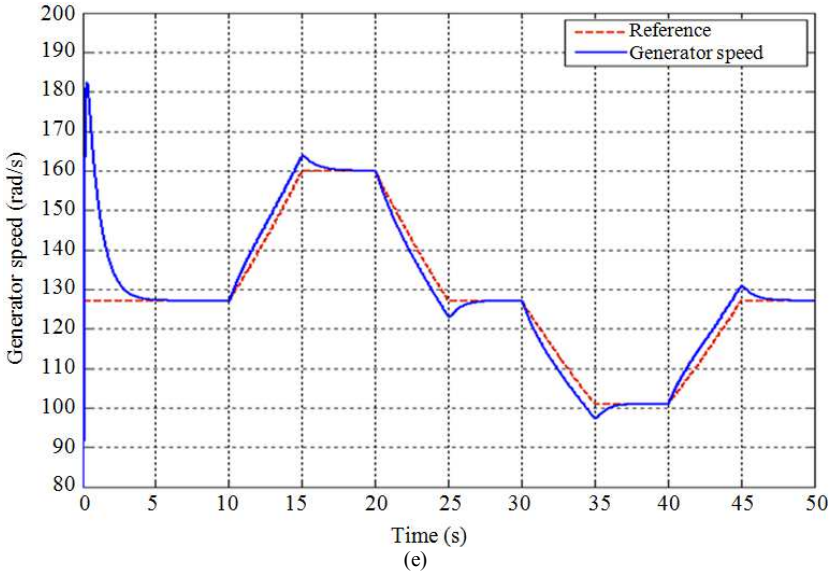
Reference
Generator speed
Generator speed (rad/s)
Time (s)

(e)

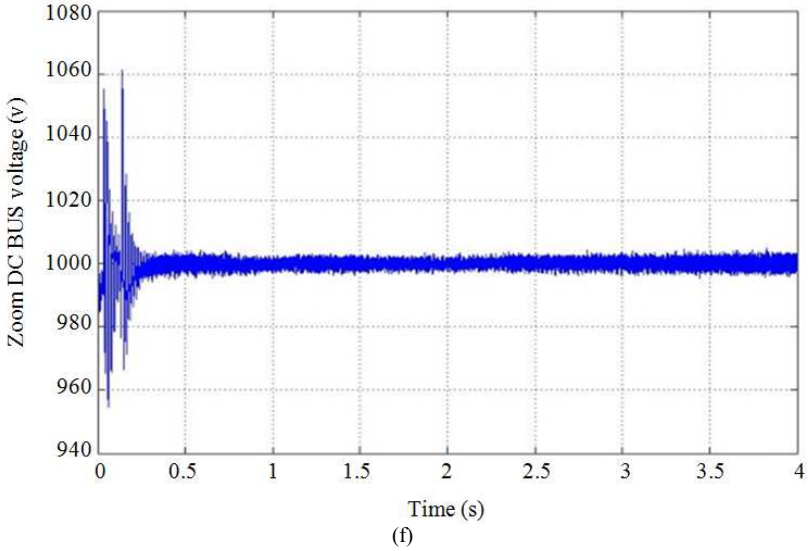
Zoom DC BUS voltage (v)
Time (s)

(f)

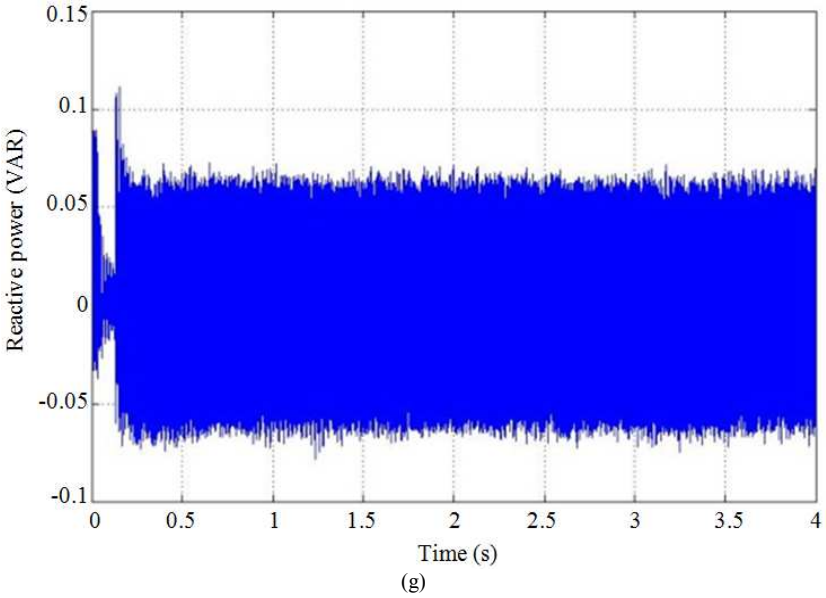

(g)

Fig. 6. Simulations results (a) Wind velocity (b) Power coefficient Cp (c) d-axis rotor flux and reference (d)Generator Power (e) Generator speed and reference (f) DC bus Voltage (g) Reactive power

Figure 6 shows the response system for a wind change velocity. Figure 6a shows the wind velocity profile imposed. Figure 6b shows the power coefficient Cp. According to this figure, the power coefficient Cp is adjusted to its optimum value (Cp = 0.5).

Figure 6c shows the d-axis rotor flux. We note that the d-axis rotor flux is regulated to its reference value (ϕ_r = 1 wb).

Figure 6d shows the mechanical power extracted from the wind power generator. According to Fig. 3, the extracted power is maximum.

Figure 6e shows the speed of the SCIG machine. We note that the speed is regulated at the reference estimated by the MPPT.

Figure 6f shows the DC bus voltage. The reference of the DC bus voltage denoted V_{dc}* is set at 1000 V. According to this figure, the DC bus voltage is regulated to its reference.

Figure 6g shows the reactive power injected to the grid. The reference value of reactive power Qg* is set to 0VAr, which guarantees a power factor close to unity. The reactive power of stator Qs is regulated to reference value.

Conclusion

This study has addressed the modeling and control of a wind system with variable speed of the wind based on a SCIG. We are interested in modeling of various components of wind system. In fact, the aerodynamic and mechanical models of the turbine have been developed. In order to establish different controllers of two converters, we have developed models of SCIG and liaison of the SCIG to the network via the inverter and RL filter.

To validate the modeling and control of the global wind system, we have performed a simulation for an operating point at variable wind speed.

According to the simulation results, the control strategy allowed regulation of the generator speed to the optimal value estimated by the MPPT algorithm. On the other hand a good decoupling between the adjustment of d-axis rotor flux and the generator speed. Finally, operating at a near-unity power factor at the injection of extracted of wind power into the grid system.

Funding Information

There is no funding for this work. this work is developed in a personal capacity

Ethics

This scientific research work is developped in the direction of improving the pruduction energitic for a global population increasingly growing and also to respond to the global economic demand.

References

Dinghui, W., L. Yuanlong and J. Zhicheng, 2009. Modeling and MPPT control of squirrel-cage induction generator wind power generation system via VisSim. Proceedings of the Chinese Control and Decision Conference, Jun. 17-19, IEEE Xplore Press, Guilin, pp: 48-53. DOI: 10.1109/CCDC.2009.5195147

Kedjar, B. and K. Al-Haddad, 2012. Optimal control of a grid connected variable speed wind energy conversion system based on squirrel cage induction generator. Proceedings of the 38th Annual Conference on IEEE Industrial Electronics Society,Oct. 25-28, IEEE Xplore Press, Montreal, QC., pp: 3560-3565. DOI: 10.1109/IECON.2012.6389327

Manaullah, M., A.K. Sharma, H. Ahuja, G. Bhuvaneswari and R. Balasubramanian, 2012. Control and dynamic analysis of grid connected variable speed SCIG based wind energy conversion system. Proceedings of the 4th International Conference on Computational Intelligence and Communication Networks, Nov. 3-5, IEEE Xplore Press, Mathura, pp: 588-593. DOI: 10.1109/CICN.2012.74

Mehdi, A., A. Boulahia, H. Medouce and H. Benalla, 2013. Induction generator using AC/DC/AC PWM converters and its application to the wind-energy systems. Proceedings of the IEEE EUROCON, Jul. 1-4, IEEE Xplore Press, Zagreb, pp: 1038-1043. DOI: 10.1109/EUROCON.2013.6625109

Mesemanolis, A. and C. Mademlis, 2013. Self-tuning maximum power point tracking control for wind generation systems. Proceedings of the International Conference on Clean Electrical Power, Jun. 11-13, IEEE Xplore Press, Alghero, pp: 407-413. DOI: 10.1109/ICCEP.2013.6587022

Suebkinorn, W., and B. Neammanee, 2011. An implementation of field oriented controlled SCIG for variable speed wind turbine. Proceedings of the 6th IEEE Conference on Industrial Electronics and Applications, Jun. 21-23, IEEE Xplore Press, Beijing, pp: 39-44. DOI: 10.1109/ICIEA.2011.5975547

Trapp, J.G., F.A. Farret, F.T. Fernandes and L.C. Correa, 2012. Variable speed wind turbine using the squirrel cage induction generator with reduced converter power rating for stand-alone energy systems. Proceedings of the 10th IEEE/IAS International Conference on Industry Applications, Nov. 5-7, IEEE Xplore Press, Fortaleza, pp: 1-8. DOI: 10.1109/INDUSCON.2012.6453324